A Method for Evaluating Resistance to Stress-Corrosion Cracking of High-Strength Aluminum Alloy by the Use of Pre-Cracked DCB Specimen

By Shuhei OHSAKI*

(Received July 16, 1979)

Abstract

This paper describes a method for evaluating the resistance to stress-corrosion cracking (SCC) in short-transverse direction of thick wrought plate of Al–Zn–Mg 7N01 alloy, using compact pre-cracked double cantilever beam (DCB) specimens.

The stress-intensity determination for the DCB specimen is performed, and a valid fracture toughness value has been obtained.

SCC growth rate da/dt as a function of K_I have been determined for the specimens with different aging treatments in a sodium chloride solution. Rankings of da/dt corresponding to region II are the same as those of the SCC resistance developed with smooth specimen data. The SCC test method by the use of the DCB specimen provides the threshold stress-intensity values K_{ISCC} and permits a more rational material characterization.

Introduction

Fracture mechanics principle and pre-cracked specimen have been applied in recent years to evaluating the resistance to stress-corrosion cracking (SCC) of high-strength materials[1)~6)]. These new methods provide a more quantitative crack growth information by utilizing the unique parameter of the stress-intensity factor K_I, characterizing the mechanical driving force at the crack tip. In addition, the use of pre-cracked specimens offers the advantage of simulating a practical situation in which flaws always exist.

The stress-corrosion crack growth rate da/dt under a given metal-environment system has been obtained as a function of K_I, with the generalized relationship as shown in **Fig. 1**. Crack growth kinetics may be devided into three regions. To determine the crack growth rate plateau at region II is significant, providing a quantitative means of comparing the resistance to SCC of alloys. If a threshold stress-intensity value K_{ISCC}, below which SCC growth does not occur, is obtained, the critical flaw depth and allowable stress level can be estimated, so that a more rational material design is permitted.

The present paper describes the method for evaluating the resistance to SCC in short-transverse direction of thick wrought plate of Al–Zn–Mg alloy, using compact pre-cracked double cantilever beam (DCB) specimens[7),8)]. The determination of the stress-intensity for the DCB specimen is presented by the experimental compliance

* Department of Mechanical Engineering, Technical College of Yamaguchi University

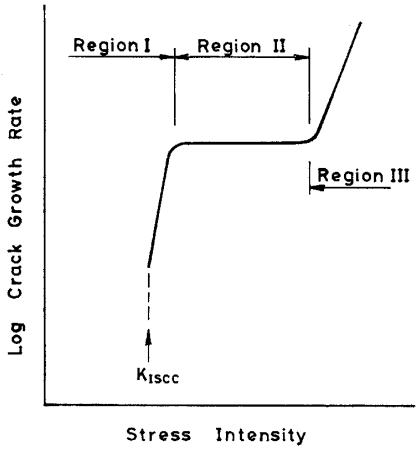

Fig. 1. Schematic illustration of the generalized relationship between stress-intensity and SCC growth rate.

method[9], and then applying this result to SCC tests the analysis of crack growth kinetics is performed.

Experimental Procedures

The present experiments employed the compact DCB specimens obtained from a 30 mm thick plate of Al–Zn–Mg 7N01 alloy. The chemical composition of this alloy is presented in **Table 1**. The dimensions of the DCB specimen and composite micrograph of the grain structure of the plate are shown in **Fig. 2**. The specimen orientation is such that stress is applied in the short-transverse direction and crack extension is in

Table 1. Chemical composition of 7NO1 aluminum alloy (wt%).

Si	Fe	Cu	Mn	Mg	Cr	Zn	Ti	Zr
0.06	0.18	0.17	0.35	1.70	0.16	4.3	0.09	0.14

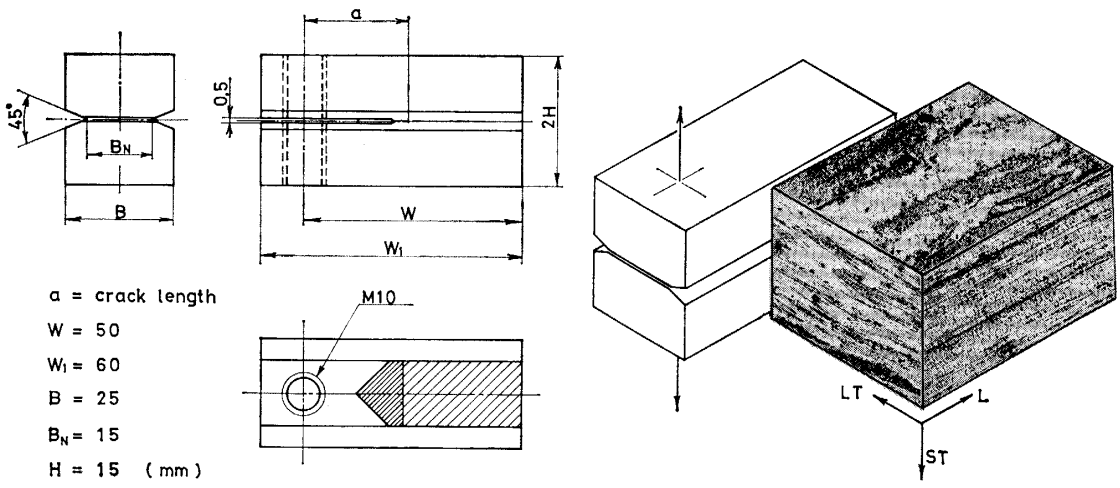

Fig. 2. Dimensions of DCB specimen and composite micrograph of the grain structure of 7N01 alloy.

the longitudinal direction. The fatigue precrack is introduced from 90-deg chevron-notch machined by grinding cutter. The side groove of the specimen is employed to provide restraints on the plastic zone at the crack tip without the formation of shear lips and to prevent crack branching.

The specimens were heat treated as follows; solid-solution treated at 465°C for one hour, quenched in 0°C water and then directly aged for given periods at various temperatures. Prior to testing, the specimen was washed by a ultrasonic cleaner, degreased with aceton followed by methanol.

For stress-intensity determination, ten above specimens with different initial precrack length, aged 24 hr at 100°C, were prepared. Compliance was determined by measuring a load-displacement curve on an X–Y recorder, in the Instron type testing machine (TENSILON UTM–25000), with cross-head speed of 0.5 mm/min. The displacement was obtained by means of a crack opening displacement (COD) gage of the clip-on type mounted on the specimen and simultaneously was monitored by photographic measurements.

The environment employed in the SCC tests is constant immersion at 30°C in an aqueous solution of 5.3% sodium chloride with the addition of 0.3% H_2O_2 and is renewed every other day. The surface of the specimen set-up on a loading rig was masked with a epoxy resin coating except the chevron notch and the side grooves. The pre-cracked section of the specimen was immersed in the corrodent using an open plastic chamber of 400 m*l*. The method of loading was with lever-type horizontal tensile-creep arrangement as shown in **Fig. 3**. Each test was conducted at a constant load with a desired initial stress-intensity level K_{Ii}. SCC growth was continuously monitored by means of the COD gage until final fracture. The electrical response of the gage was recorded by means of a strip chart recorder, and converted to COD value by a prior calibration of the gage. The displacement values were then converted to crack length by using compliance relationship. The stress-intensity factors corresponding to initial and final deta points were checked by making a survey of crack lengths on the fracture surface after rupture.

All the calculations were performed by utilizing a table of figures calculated by the computer.

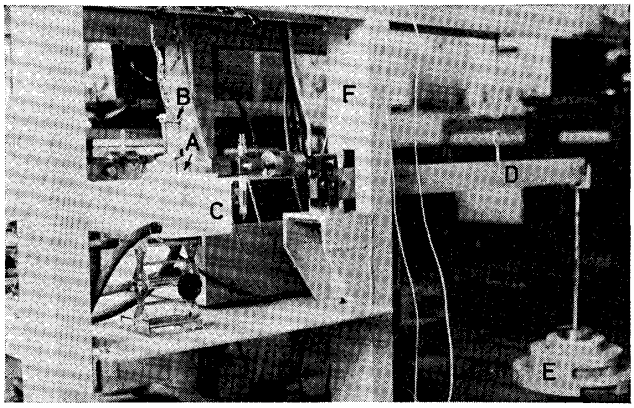

Fig. 3. Arrangement for SCC test.
A Specimen clamped with loading rig
B Clip-on type COD gage
C Environment chamber
D Lever arm
E Weight
F Test stand

Results and Discussion

Stress-Intensity Determination

The load-displacement diagrams for the DCB specimens with different precrack lengths are shown in **Fig. 4**, consisting of an autographic plot of the output of the load cell versus the output of the COD gage. Popin, followed by unstable crack extension, is observed below the load P_Q which is indicated as the intersection of the secant line with slope 5% less than the initial slope of the record, according to ASTM Method E399–78. The plane fracture toughness value K_{IC} may be presented later corresponding to P_Q.

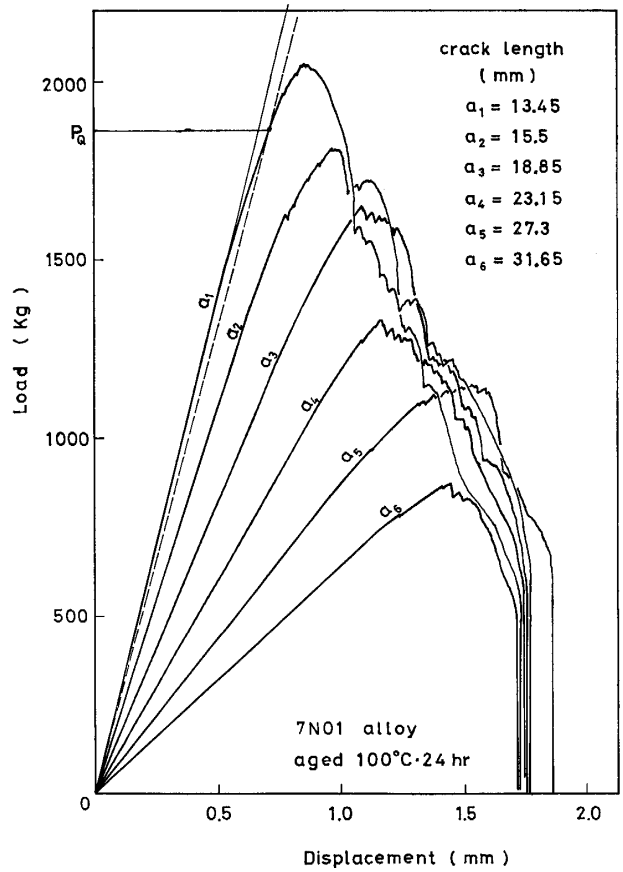

Fig. 4. Load-displacement (output of the COD gage) diagrams.

An example of the COD measured photographically as a function of the position on the specimen is shown in **Fig. 5**. From this figure, the COD measurement obtained as output of the gage can be converted to the COD values at the point of the load application, by linear interpolation, because the crack tip may be regarded as a fixed center of rotation of the beam.

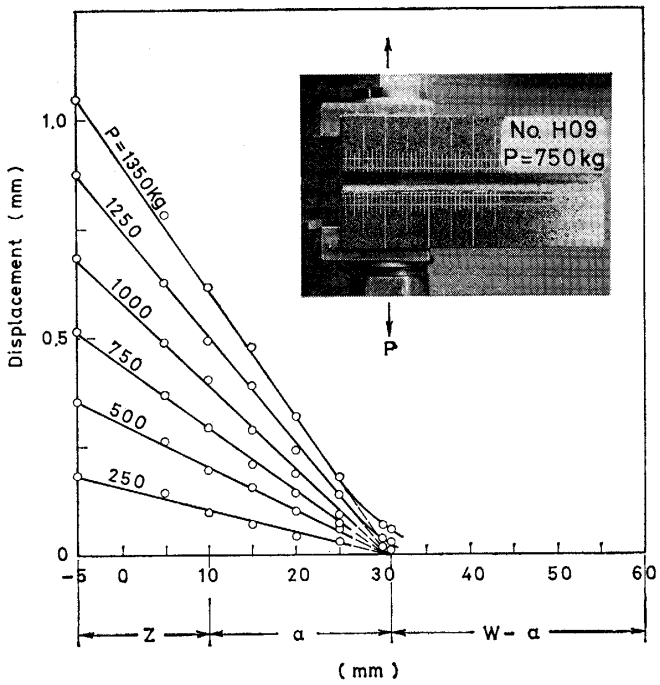

Fig. 5. COD measured photographically as a function of the position.

The compliance calibration data are obtained in the relationship of equation (1), over a crack length-to-specimen width (a/W) range of $0.19 \sim 0.63$, as shown in **Fig. 6.**

$$\Phi = EI(\delta/P) \tag{1}$$

where

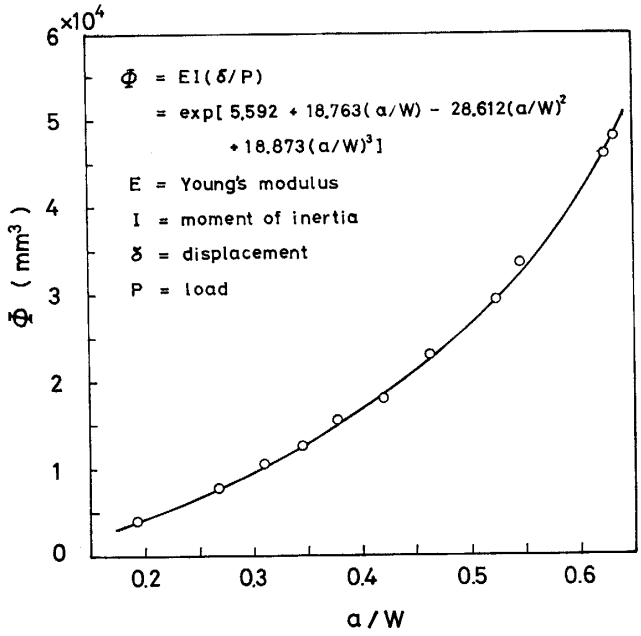

Fig. 6. Compliance as a function of crack length for DCB specimens.

P=load, Kg

δ =COD at the point of load application, mm

E=Young's modulus, 7×10^3 Kg/mm^2

I =moment of inertia of one arm with beam depth H, mm.

Using a least squares analysis, the following equation is fit to the data

$$\Phi=\exp\,[5.592+18.763(a/W)-28.612(a/W)^2+18.873(a/W)^3] \tag{2}$$

The strain energy release rate G can be given as follows

$$G=\frac{P^2}{2B_NEI}\left(\frac{d\Phi}{da}\right) \tag{3}$$

where B_N=net specimen thickness between side groove, mm, and then may be converted to the stress-intensity factor K_I using the relationship

$$K_I=\left(\frac{EG}{1-\mu^2}\right)^{1/2} \tag{4}$$

for plane strain conditions, where μ is Poisson's ratio 0.33. The stress-intensity factor corresponding to any crack length can be readily determined by means of these equations. K_I/P versus a/W plot is presented in **Fig. 7**.

Using the K_I calibration results, the fracture toughness values K_{IC} were estimated from the loads P_Q in the previous data of the specimens aged 24 hr at 100°C. The

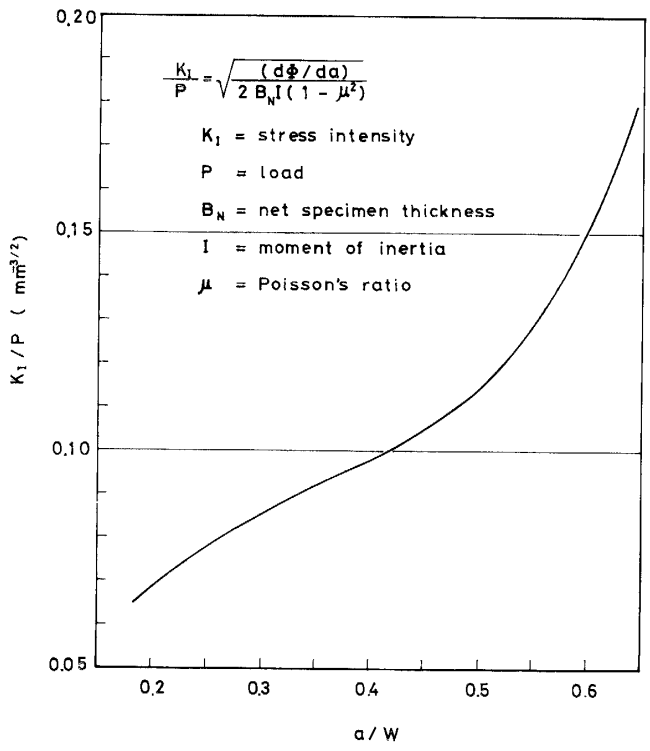

Fig. 7. Stress-intensity per unit load as a function of crack length for DCB specimen.

results are shown in **Fig. 8**, exhibiting approximately constant value $K_{IC}=140$ Kg/mm$^{3/2}$, independent of crack length. Therefore it can be considered that the result of K_I calibration is accepted as valid enough to be applicable to examining SCC kinetics.

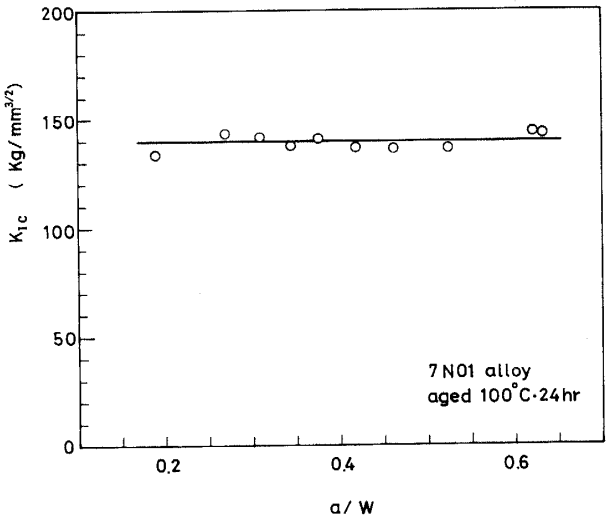

Fig. 8. Fracture toughness results as a function of crack length for 7NO1 alloy aged 24 hr at 100°C.

SCC Test

SCC tests were performed on the DCB specimens with various aging treatments, that is, aged 24 hr at 60°, 85°, 100° and 120°C respectively and naturally aged for 2 months. **Fig. 9** shows the times to terminal rupture as a function of the initial applied stress-intensity K_{Ii}. The curve on a series of the aged specimens may be of the same general shape, the failure time gradually increasing with decreasing K_{Ii}. The threshold level K_{ISCC}, with the curve becoming horizontal, appears to exist. The K_{ISCC} value of the specimen aged 24 hr at 60°C seems to be at least 30 Kg/mm$^{3/2}$. When the specimen loaded at $K_{Ii}=30$ Kg/mm$^{3/2}$ for 1000 hr was taken out of the solution, broken, and examined, no SCC growth was observed at all. The K_{ISCC} level of the specimen aged 24 hr at 100°C reveals to be a little higher than that of 60°C aging. On comparing the failure times at about a same level $K_{Ii}\approx 75$ Kg/mm$^{3/2}$, the specimen aged at the higher temperature has clearly the longer lifetime. Among these the naturally aged specimen is most sensitive to SCC. It is recognized that rankings of the resistance to SCC with aging treatments are the same as the results[10] obtained on smooth specimen by constant-strain SCC test method.

Typical plots of COD (output of the gage) as a function of time are shown in **Fig. 10**, for one of the specimen aged 24 hr at 100°C, with lifetime of about 250 hr. Crack length a, is converted from each COD data point by means of the compliance relationship, and instantanious values of K_I are plotted in this figure. As the crack grows from initial crack length $a_0=21.4$ mm to final crack length $a_f=33.5$ mm, K_I value increases from $K_{Ii}=77.2$ Kg/mm$^{3/2}$ until it attains the critical value for fast

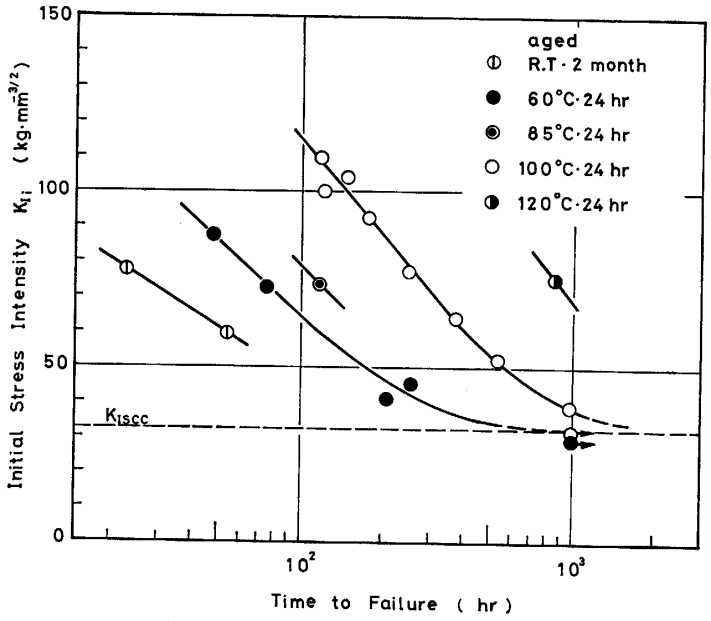

Fig. 9. Time to failure as a function of the initial applied stress-intensity for 7NO1 alloys.

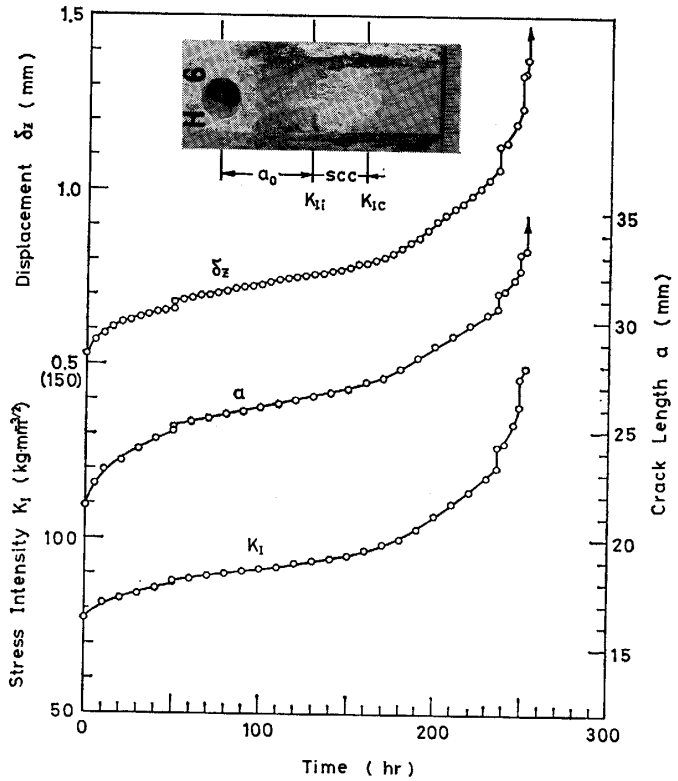

Fig. 10. Typical COD-, crack length- and stress-intensity-time plots for DCB specimen aged 24 hr at 100°C.

fracture which is approximately equal to the previous K_{IC} value. The occurrence of crack extension on loading, followed by transient growth, is observed. Following the

initial transient growth, the crack appears to enter the steady-stage of growth. This nonsteady-state growth period may be affected by K_{Ii} level as the observations by Landes and Wei[11].

The SCC growth rate da/dt is determined by calculating the slope of the crack length-time curve. Steady-state crack growth responses as a function of K_I are presented in **Fig. 11**. da/dt–K_I plots have the same general shape with distinguishable region II and region III, except that of the naturally aged specimen. Region II is independent of K_I, with one- or two-plateaus of da/dt, and represents a range where crack growth may be limited by the embrittling chemical process, involving mass transport. Popin with audible acoustic emission is often observed at the time when da/dt transfers from the lower plateau to the higher one. In region III, da/dt increases rapidly with increasing K_I, approaching the condition for the onset of fast fracture. It is clearly found that the specimen aged at the higher temperature has the lower da/dt at $K_I \approx 100$ Kg/mm$^{3/2}$ of region II. T4 specimen (naturally aged for 2 months) is very sensitive to SCC, having as about 100-times high da/dt as that of T6 specimen (aged for 24 hr at 120°C).

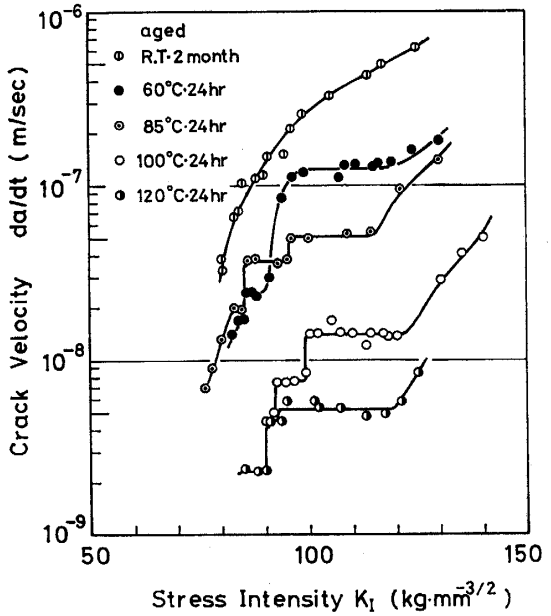

Fig. 11. SCC growth rate versus stress intensity for aged 7NO1 alloys.

Fig. 12 shows the fracture surfaces of T4 and T6 specimens. The upper and lower views are by optical microscope and scanning electron microscope (SEM) respectively. The SEM view of T4 specimen appears intergranular SCC fracture of smooth and featureless aspects, with less mechanical rupturing. In the optical micrograph, however, laminated tongues are frequently found, representing that a crack plane consisted of platelike-elongated grain boundary may readily shift to either just above or below grain boundary plane. So SCC certainly grows with giving rise to

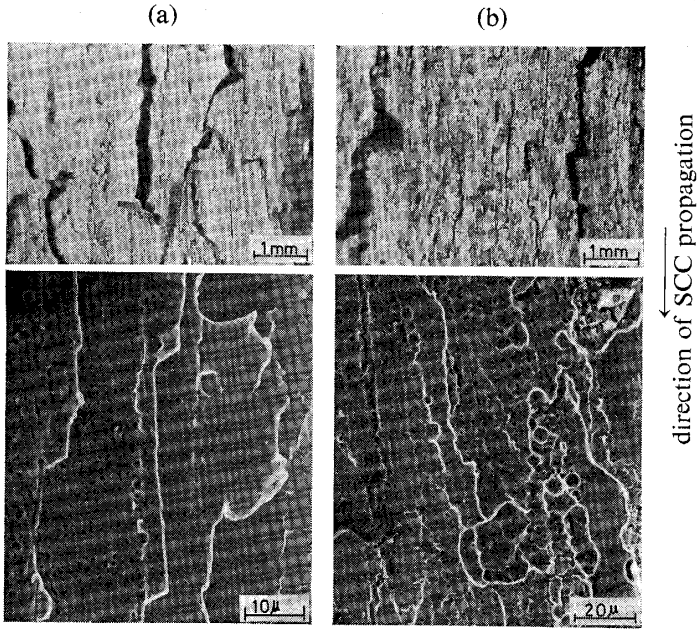

(a) aged R.T×2 month, $K_{Ii}=74.8$ kg·mm$^{-3/2}$
(b) aged 120°C×24 hr, $K_{Ii}=75.6$ kg·mm$^{-3/2}$

Fig. 12. Fractographs of SCC ruptured specimens.

micro-branching in terms of microstructure. T6 specimen of the higher resistance to SCC, in spite of less micro-branching, shows intergranular fracture surface of uneven aspects, involving parts of dimple. The fractographs of T6 specimen suggest that it is hard for effective path to SCC propagation to be formed from a viewpoint of state of grain boundary precipitation.

Summary

In order to evaluate the resistance to SCC in short-transverse direction of thick wrought plate of Al–Zn–Mg 7N01 alloy, using fracture mechanics approach, a more compact DCB specimen has been designed. The stress-intensity K_I calibration for the DCB specimen was performed by experimental determination of compliance, and provided a valid fracture toughness value.

The DCB specimen is applied to environment tests in an aqueous sodium chloride solution for determining the SCC kinetics of alloys with different aging treatments. Crack length a versus time t curves and SCC growth rate da/dt versus K_I curves are obtained for each aged alloy, representing a general shape with region II and region III. Rankings of da/dt corresponding to region II are the same as those of the SCC resistance developed with smooth specimen data. That is, da/dt decreasing with increasing aging temperature for a given aging time. T4 specimen has as about 100-times high da/dt as that of T6 specimen. These results are correspondent well with fractographic observations by SEM.

The SCC method by the use of the DCB specimen provides the threshold stress-

intensity values K_{ISCC} too, and then is useful to permit a more rational material characterization.

Acknowledgments

The author would like to thank Prof. T. Takahashi, Dr. Y. Kojima of Tokyo Institute of Technology, and Prof. S. Shimizu of Yamaguchi University for helpful suggestions during the course of this research. He would like to gratefully acknowledge the computer analysis provided by associate Prof. Y. Ishihara of Technical College of Yamaguchi University.

References

1) B. F. Brown and C. D. Beachem, Corrosion Sci., **5**, 745 (1965)
2) B. F. Brown, Material Research & Standards, **6**, 129 (1966)
3) B. F. Brown, Metallurgical Reviews, **129**, 171 (1968)
4) S. R. Novak and S. T. Rolfe, J. of Materials, **14**, 701 (1969)
5) J. H. Mulherin, Stress Corrosion Testing, ASTM STP 425, 66 (1967)
6) A. A. Sheinker and J. D. Wood, Stress Corrosion Cracking of Metals — A State of the Art., ASTM STP 518, 16 (1971)
7) M. O. Speidel, Metallurgical Transactions, **6A**, 631 (1975)
8) D. O. Sprowls, J. W. Coursen, and J. D. Walsh, Stress Corrosion — New Approaches, ASTM STP 610, 143 (1976)
9) R. G. Hoagland, Transactions of ASME, J. of Basic Engineering, 525 (1967)
10) T. Takahashi, Y. Kojima and S. Ohsaki, Preprint of Japan Institute of Light Metals, **56**, 37 (1979)
11) R. P. Wei, S. R. Novak, and D. P. Williams, Materials Research and Standards, **12**, 25 (1972)